



KEK preprint 2001-xx  
BELLE preprint 2001-xx

# A Measurement of Lifetime Difference in $D^0$ Meson Decays

The Belle Collaboration  
(November 8, 2001)

## Abstract

We report a measurement of the  $D^0$ - $\bar{D}^0$  mixing parameter  $y_{CP}$  using  $23.4 \text{ fb}^{-1}$  of data collected near the  $\Upsilon(4S)$  resonance with the Belle detector at KEKB.  $y_{CP}$  is measured from the lifetime difference of  $D^0$  mesons decaying into the  $K^-\pi^+$  state and the  $CP$  even eigenstate  $K^-K^+$ . We find  $y_{CP} = (-0.5 \pm 1.0_{-0.8}^{+0.7}) \times 10^{-2}$ , where the first error is statistical and the second systematic, corresponding to a 95% confidence interval  $-0.030 < y_{CP} < 0.020$ .

PACS numbers: 12.15.Ff,13.25.Ft,14.40.Lb

arXiv:hep-ex/0111026v1 8 Nov 2001

Typeset using REVTeX

K. Abe<sup>8</sup>, K. Abe<sup>42</sup>, R. Abe<sup>31</sup>, T. Abe<sup>43</sup>, I. Adachi<sup>8</sup>, Byoung Sup Ahn<sup>16</sup>, H. Aihara<sup>44</sup>, M. Akatsu<sup>24</sup>, Y. Asano<sup>49</sup>, T. Aso<sup>48</sup>, V. Aulchenko<sup>2</sup>, T. Aushev<sup>13</sup>, A. M. Bakich<sup>40</sup>, Y. Ban<sup>35</sup>, S. Behari<sup>8</sup>, P. K. Behera<sup>50</sup>, A. Bondar<sup>2</sup>, A. Bozek<sup>29</sup>, T. E. Browder<sup>7</sup>, B. C. K. Casey<sup>7</sup>, Y. Chao<sup>28</sup>, B. G. Cheon<sup>39</sup>, R. Chistov<sup>13</sup>, Y. Choi<sup>39</sup>, L. Y. Dong<sup>11</sup>, S. Eidelman<sup>2</sup>, V. Eiges<sup>13</sup>, F. Fang<sup>7</sup>, H. Fujii<sup>8</sup>, C. Fukunaga<sup>46</sup>, M. Fukushima<sup>10</sup>, N. Gabyshev<sup>8</sup>, A. Garmash<sup>2,9</sup>, T. Gershon<sup>8</sup>, A. Gordon<sup>22</sup>, R. Guo<sup>26</sup>, J. Haba<sup>8</sup>, H. Hamasaki<sup>8</sup>, K. Hanagaki<sup>36</sup>, F. Handa<sup>43</sup>, K. Hara<sup>33</sup>, T. Hara<sup>33</sup>, N. C. Hastings<sup>22</sup>, H. Hayashii<sup>25</sup>, M. Hazumi<sup>33</sup>, E. M. Heenan<sup>22</sup>, I. Higuchi<sup>43</sup>, T. Higuchi<sup>44</sup>, T. Hojo<sup>33</sup>, T. Hokuue<sup>24</sup>, Y. Hoshi<sup>42</sup>, K. Hoshina<sup>47</sup>, S. R. Hou<sup>28</sup>, W.-S. Hou<sup>28</sup>, S.-C. Hsu<sup>28</sup>, H.-C. Huang<sup>28</sup>, Y. Igarashi<sup>8</sup>, T. Iijima<sup>8</sup>, H. Ikeda<sup>8</sup>, K. Inami<sup>24</sup>, A. Ishikawa<sup>24</sup>, H. Ishino<sup>45</sup>, R. Itoh<sup>8</sup>, H. Iwasaki<sup>8</sup>, Y. Iwasaki<sup>8</sup>, P. Jalocha<sup>29</sup>, H. K. Jang<sup>38</sup>, J. H. Kang<sup>53</sup>, J. S. Kang<sup>16</sup>, N. Katayama<sup>8</sup>, H. Kawai<sup>3</sup>, H. Kawai<sup>44</sup>, N. Kawamura<sup>1</sup>, T. Kawasaki<sup>31</sup>, H. Kichimi<sup>8</sup>, D. W. Kim<sup>39</sup>, Heejong Kim<sup>53</sup>, H. J. Kim<sup>53</sup>, H. O. Kim<sup>39</sup>, Hyunwoo Kim<sup>16</sup>, T. H. Kim<sup>53</sup>, K. Kinoshita<sup>5</sup>, S. Kobayashi<sup>37</sup>, H. Konishi<sup>47</sup>, S. Korpar<sup>21,14</sup>, P. Križan<sup>20,14</sup>, P. Krokovny<sup>2</sup>, R. Kulasiri<sup>5</sup>, S. Kumar<sup>34</sup>, A. Kuzmin<sup>2</sup>, Y.-J. Kwon<sup>53</sup>, J. S. Lange<sup>6</sup>, G. Leder<sup>12</sup>, S. H. Lee<sup>38</sup>, D. Liventsev<sup>13</sup>, J. MacNaughton<sup>12</sup>, D. Marlow<sup>36</sup>, T. Matsubara<sup>44</sup>, S. Matsumoto<sup>4</sup>, T. Matsumoto<sup>24</sup>, Y. Mikami<sup>43</sup>, K. Miyabayashi<sup>25</sup>, H. Miyake<sup>33</sup>, H. Miyata<sup>31</sup>, G. R. Moloney<sup>22</sup>, S. Mori<sup>49</sup>, T. Mori<sup>4</sup>, A. Murakami<sup>37</sup>, T. Nagamine<sup>43</sup>, Y. Nagasaka<sup>9</sup>, Y. Nagashima<sup>33</sup>, T. Nakadaira<sup>44</sup>, E. Nakano<sup>32</sup>, M. Nakao<sup>8</sup>, J. W. Nam<sup>39</sup>, Z. Natkaniec<sup>29</sup>, K. Neichi<sup>42</sup>, S. Nishida<sup>17</sup>, O. Nitoh<sup>47</sup>, S. Noguchi<sup>25</sup>, T. Nozaki<sup>8</sup>, S. Ogawa<sup>41</sup>, T. Ohshima<sup>24</sup>, T. Okabe<sup>24</sup>, S. Okuno<sup>15</sup>, S. L. Olsen<sup>7</sup>, W. Ostrowicz<sup>29</sup>, H. Ozaki<sup>8</sup>, P. Pakhlov<sup>13</sup>, H. Palka<sup>29</sup>, C. S. Park<sup>38</sup>, C. W. Park<sup>16</sup>, H. Park<sup>18</sup>, K. S. Park<sup>39</sup>, J.-P. Perroud<sup>19</sup>, M. Peters<sup>7</sup>, L. E. Pilonen<sup>51</sup>, J. L. Rodriguez<sup>7</sup>, N. Root<sup>2</sup>, M. Rozanska<sup>29</sup>, K. Rybicki<sup>29</sup>, H. Sagawa<sup>8</sup>, Y. Sakai<sup>8</sup>, H. Sakamoto<sup>17</sup>, M. Satpathy<sup>50</sup>, A. Satpathy<sup>9,5</sup>, S. Schrenk<sup>5</sup>, S. Semenov<sup>13</sup>, K. Senyo<sup>24</sup>, M. E. Sevier<sup>22</sup>, H. Shibuya<sup>41</sup>, B. Shwartz<sup>2</sup>, J. B. Singh<sup>34</sup>, S. Stanić<sup>49</sup>, K. Sumisawa<sup>8</sup>, T. Sumiyoshi<sup>8</sup>, S. Suzuki<sup>52</sup>, S. Y. Suzuki<sup>8</sup>, S. K. Swain<sup>7</sup>, H. Tajima<sup>44</sup>, T. Takahashi<sup>32</sup>, F. Takasaki<sup>8</sup>, M. Takita<sup>33</sup>, K. Tamai<sup>8</sup>, N. Tamura<sup>31</sup>, J. Tanaka<sup>44</sup>, M. Tanaka<sup>8</sup>, Y. Tanaka<sup>23</sup>, Y. Teramoto<sup>32</sup>, M. Tomoto<sup>8</sup>, T. Tomura<sup>44</sup>, S. N. Tovey<sup>22</sup>, K. Trabelsi<sup>7</sup>, T. Tsuboyama<sup>8</sup>, T. Tsukamoto<sup>8</sup>, S. Uehara<sup>8</sup>, K. Ueno<sup>28</sup>, Y. Unno<sup>3</sup>, S. Uno<sup>8</sup>, Y. Ushiroda<sup>8</sup>, K. E. Varvell<sup>40</sup>, C. C. Wang<sup>28</sup>, C. H. Wang<sup>27</sup>, J. G. Wang<sup>51</sup>, M.-Z. Wang<sup>28</sup>, Y. Watanabe<sup>45</sup>, E. Won<sup>38</sup>, B. D. Yabsley<sup>8</sup>, Y. Yamada<sup>8</sup>, M. Yamaga<sup>43</sup>, A. Yamaguchi<sup>43</sup>, H. Yamamoto<sup>43</sup>, Y. Yamashita<sup>30</sup>, M. Yamauchi<sup>8</sup>, M. Yokoyama<sup>44</sup>, K. Yoshida<sup>24</sup>, Y. Yusa<sup>43</sup>, C. C. Zhang<sup>11</sup>, J. Zhang<sup>49</sup>, Y. Zheng<sup>7</sup>, V. Zhilich<sup>2</sup>, and D. Žontar<sup>49</sup>

<sup>1</sup>Aomori University, Aomori

<sup>2</sup>Budker Institute of Nuclear Physics, Novosibirsk

<sup>3</sup>Chiba University, Chiba

<sup>4</sup>Chuo University, Tokyo

<sup>5</sup>University of Cincinnati, Cincinnati OH

<sup>6</sup>University of Frankfurt, Frankfurt

<sup>7</sup>University of Hawaii, Honolulu HI

<sup>8</sup>High Energy Accelerator Research Organization (KEK), Tsukuba

<sup>9</sup>Hiroshima Institute of Technology, Hiroshima

<sup>10</sup>Institute for Cosmic Ray Research, University of Tokyo, Tokyo

<sup>11</sup>Institute of High Energy Physics, Chinese Academy of Sciences, Beijing

<sup>12</sup>Institute of High Energy Physics, Vienna

- <sup>13</sup>Institute for Theoretical and Experimental Physics, Moscow  
<sup>14</sup>J. Stefan Institute, Ljubljana  
<sup>15</sup>Kanagawa University, Yokohama  
<sup>16</sup>Korea University, Seoul  
<sup>17</sup>Kyoto University, Kyoto  
<sup>18</sup>Kyungpook National University, Taegu  
<sup>19</sup>IPHE, University of Lausanne, Lausanne  
<sup>20</sup>University of Ljubljana, Ljubljana  
<sup>21</sup>University of Maribor, Maribor  
<sup>22</sup>University of Melbourne, Victoria  
<sup>23</sup>Nagasaki Institute of Applied Science, Nagasaki  
<sup>24</sup>Nagoya University, Nagoya  
<sup>25</sup>Nara Women's University, Nara  
<sup>26</sup>National Kaohsiung Normal University, Kaohsiung  
<sup>27</sup>National Lien-Ho Institute of Technology, Miao Li  
<sup>28</sup>National Taiwan University, Taipei  
<sup>29</sup>H. Niewodniczanski Institute of Nuclear Physics, Krakow  
<sup>30</sup>Nihon Dental College, Niigata  
<sup>31</sup>Niigata University, Niigata  
<sup>32</sup>Osaka City University, Osaka  
<sup>33</sup>Osaka University, Osaka  
<sup>34</sup>Panjab University, Chandigarh  
<sup>35</sup>Peking University, Beijing  
<sup>36</sup>Princeton University, Princeton NJ  
<sup>37</sup>Saga University, Saga  
<sup>38</sup>Seoul National University, Seoul  
<sup>39</sup>Sungkyunkwan University, Suwon  
<sup>40</sup>University of Sydney, Sydney NSW  
<sup>41</sup>Toho University, Funabashi  
<sup>42</sup>Tohoku Gakuin University, Tagajo  
<sup>43</sup>Tohoku University, Sendai  
<sup>44</sup>University of Tokyo, Tokyo  
<sup>45</sup>Tokyo Institute of Technology, Tokyo  
<sup>46</sup>Tokyo Metropolitan University, Tokyo  
<sup>47</sup>Tokyo University of Agriculture and Technology, Tokyo  
<sup>48</sup>Toyama National College of Maritime Technology, Toyama  
<sup>49</sup>University of Tsukuba, Tsukuba  
<sup>50</sup>Utkal University, Bhubaneswer  
<sup>51</sup>Virginia Polytechnic Institute and State University, Blacksburg VA  
<sup>52</sup>Yokkaichi University, Yokkaichi  
<sup>53</sup>Yonsei University, Seoul

The search for  $D^0$ - $\bar{D}^0$  mixing provides an important window on physics beyond the Standard Model (SM). Since the predicted rate of mixing in the SM is very small [1], large mixing could indicate a contribution from non-SM processes. One measure of mixing effects is the difference in decay rate between the  $CP$  even and  $CP$  odd eigenstates of the system, parameterized by

$$y_{CP} \equiv \frac{\hat{\Gamma}(CP \text{ even}) - \hat{\Gamma}(CP \text{ odd})}{\hat{\Gamma}(CP \text{ even}) + \hat{\Gamma}(CP \text{ odd})},$$

where  $\hat{\Gamma}$  is the effective decay rate obtained by fitting a single exponential to the measured decay distribution for each final state [2]. We combine decays from  $D^0$  and  $\bar{D}^0$ , which we assume to be produced at equal rates in  $e^+e^-$  collisions. Using the  $K^-K^+$  final state (a  $CP$ -even eigenstate) and the  $K^-\pi^+$  final state (which is not a  $CP$  eigenstate) [3], we measure  $y_{CP}$  as  $\tau(K^-\pi^+)/\tau(K^-K^+) - 1$ , where  $\tau = 1/\hat{\Gamma}$ . The parameter  $y_{CP}$  can be expressed as  $y_{CP} = y \cos \phi + x \Delta \sin \phi$  [4]. Here  $x = (M_1 - M_2)/\Gamma_{\text{av}}$  and  $y = (\Gamma_1 - \Gamma_2)/2\Gamma_{\text{av}}$ , where  $M_{1,2}$  and  $\Gamma_{1,2}$  are the masses and decay widths for the  $|D_{1,2}\rangle = p|D^0\rangle \pm q|\bar{D}^0\rangle$  physical states of the neutral  $D$  meson system, and  $\Gamma_{\text{av}} = \frac{1}{2}(\Gamma_1 + \Gamma_2)$ .  $\Delta$ ,  $|\alpha| - 1$ , and  $\phi$  are  $CP$  violating parameters:  $\Delta = (|p|^2 - |q|^2)/(|p|^2 + |q|^2)$ ,  $\alpha = q\mathcal{A}(\bar{D}^0 \rightarrow K^-K^+)/p\mathcal{A}(D^0 \rightarrow K^-K^+)$ , and  $\phi = \arg(\alpha)$ , where  $\mathcal{A}(D^0(\bar{D}^0) \rightarrow K^-K^+)$  are the decay amplitudes. The above expression for  $y_{CP}$  is correct to first order in  $x$ ,  $y$ ,  $\Delta$  and  $|\alpha| - 1$ ; in the  $CP$ -conserving limit,  $y_{CP} = y$ .

The FOCUS collaboration recently reported  $y_{CP} = (3.42 \pm 1.39 \pm 0.74) \times 10^{-2}$  [5]. Since the SM prediction is  $x, y \sim O(10^{-3})$ , and non-SM processes are expected to manifest themselves as a large value of  $x$ , such a large value for  $y_{CP}$  could be interpreted as a failure of the SM prediction [6]. We note that limits on the mixing parameter  $x$  are weak ( $|x| < 0.03 \sim 0.06$ ), and the asymmetry parameter  $\Delta$  is not constrained by existing measurements [7], so that a large  $y_{CP}$  could also be accommodated if  $CP$  violating effects were large.

In this Letter, we present a new measurement of  $y_{CP}$  with better statistical precision than the FOCUS result and largely independent systematic errors. The data sample for this analysis corresponds to an integrated luminosity of  $20.9 \text{ fb}^{-1}$  taken at the  $\Upsilon(4S)$  resonance and of  $2.5 \text{ fb}^{-1}$  taken 60 MeV below the  $\Upsilon(4S)$  resonance collected with the Belle detector at the KEKB collider. KEKB [8] is an asymmetric energy electron-positron collider designed to produce boosted  $B$  mesons. The electron and positron beam energies are 8 GeV and 3.5 GeV, respectively: the resulting energy in the center-of-mass system (cms), 10.58 GeV, corresponds to the mass of the  $\Upsilon(4S)$  resonance.

The Belle detector [9] consists of a three-layer double-sided ( $r\phi$  and  $rz$  planes) silicon vertex detector (SVD), a 50-layer central drift chamber (CDC), an array of 1188 aerogel Čerenkov counters (ACC), 128 time-of-flight (TOF) scintillation counters, an electromagnetic calorimeter containing 8736 CsI(Tl) crystals and 14 layers of 4.7-cm-thick iron plates interleaved with a system of resistive plate counters (KLM). All subdetectors except the KLM are located inside a 3.4 m diameter superconducting solenoid which provides a 1.5 Tesla magnetic field. The impact parameter resolutions for charged tracks are measured to be  $\sigma_{xy}^2 = (19)^2 + (50/(p\beta \sin^{3/2} \theta))^2 \mu\text{m}^2$  in the plane perpendicular to the beam ( $z$ ) axis and  $\sigma_z^2 = (36)^2 + (42/(p\beta \sin^{5/2} \theta))^2 \mu\text{m}^2$  along the  $z$  axis, where  $\beta = p/E$ ,  $p$  and  $E$  are the momentum (GeV/ $c$ ) and energy (GeV), and  $\theta$  is the polar angle from the  $z$  axis. The transverse momentum resolution is  $(\sigma_{p_T}/p_T)^2 = (0.0019p_T)^2 + (0.0030)^2$ , where  $p_T$  is in GeV/ $c$ .

Candidate  $D^0$  mesons [10] are reconstructed via  $D^0 \rightarrow K^-\pi^+$  and  $D^0 \rightarrow K^-K^+$  decays. We require candidate charged tracks to be well reconstructed, and associated with at least two

SVD hits in both the  $r\phi$  and  $rz$  planes. Charged pion and kaon candidates are selected based on a particle identification likelihood value calculated using CDC energy loss measurements, flight times measured in the TOF, and the response of the ACC; for the chosen cuts,  $K^\pm$  are identified with an efficiency of  $\sim 85\%$  and a charged pion fake rate of  $\sim 10\%$  for all momenta up to  $3.5 \text{ GeV}/c$ . A  $D^0$  candidate is required to have cms momentum greater than  $2.5 \text{ GeV}/c$  to eliminate secondary  $D^0$  mesons originating from  $B\bar{B}$  events. To suppress the background due to random combinations of two oppositely charged tracks, a cut is imposed on the decay angle  $\theta_D$  defined as the angle between the momentum vector of the  $D^0$  candidate in the laboratory frame and that of the  $\pi^+$  ( $K^+$ ) in the  $D^0$  rest frame for the  $K^-\pi^+$  ( $K^-K^+$ ) decay:  $\cos\theta_D > -0.85$  for the  $K^-\pi^+$  decay and  $|\cos\theta_D| < 0.90$  for the  $K^-K^+$  decay, where the  $\cos\theta_D$  distribution is expected to be flat for signal. The two tracks forming the  $D^0$  candidate are required to originate from a common vertex. In addition, the reconstructed  $D^0$  flight path is required to be consistent with originating at the  $e^+e^-$  interaction point (IP) profile. Figure 1 shows invariant mass distributions for  $D^0 \rightarrow K^-\pi^+$  and  $D^0 \rightarrow K^-K^+$  candidates, superimposed with the result of a fit with two Gaussians (for signal) plus a linear function (for background). We find  $214260 \pm 562$   $D^0 \rightarrow K^-\pi^+$  and  $18306 \pm 189$   $D^0 \rightarrow K^-K^+$  signal events, as determined from the area of the two Gaussians. The signal purity in the mass region within  $3\sigma$  of the measured mean  $D^0$  mass is  $87\%$  for  $K^-\pi^+$  ( $67\%$  for  $K^-K^+$ ), where  $\sigma$  is the weighted average of the standard deviations of two Gaussians and is  $6.5 \text{ MeV}/c^2$  ( $5.4 \text{ MeV}/c^2$  for  $K^-K^+$ ).

The decay vertex ( $\mathbf{x}_{\text{dec}}$ ) of the charm meson is determined using both tracks that form the charm meson candidate. The production vertex ( $\mathbf{x}_{\text{pro}}$ ) is obtained by extrapolating the  $D^0$  flight path to the IP. The center and size of the IP profile are determined for each KEKB fill [11]. The IP size is  $\sigma_x = (80 - 120) \mu\text{m}$ ,  $\sigma_y = (2 - 4) \mu\text{m}$ , and  $\sigma_z = (3 - 4) \text{ mm}$ . The projected decay length ( $\ell$ ) in 3-dimensional space and the proper-time ( $t$ ) are obtained from  $\ell = (\mathbf{x}_{\text{dec}} - \mathbf{x}_{\text{pro}}) \cdot \mathbf{p}_D / |\mathbf{p}_D|$  and  $t = \ell m_D / c |\mathbf{p}_D|$ , respectively, where  $\mathbf{p}_D$  and  $m_D$  are the momentum vector of the reconstructed charm meson and the world average value of the  $D^0$  mass [12]. The selected  $D^0$  mesons have a laboratory momentum of  $3.6 \text{ GeV}/c$  and a decay length of  $\sim 200 \mu\text{m}$  on average. A Monte Carlo (MC) simulation study indicates that the decay and production vertex resolutions along the  $D^0$  flight direction are  $110 \mu\text{m}$  (rms) and  $70 \mu\text{m}$  (rms), respectively. We reject a small fraction ( $\sim 3\%$ ) of the  $D^0$  candidates by requiring that the uncertainty of the decay length measurement be less than  $300 \mu\text{m}$ .

In this analysis we extract the value of  $y_{CP}$  by combining likelihood functions for  $D^0 \rightarrow K^-\pi^+$  and  $D^0 \rightarrow K^-K^+$  decays,

$$L_{y_{CP}} = L_{K^-\pi^+} \cdot L_{K^-K^+},$$

and expressing the lifetime for  $D^0 \rightarrow K^-K^+$  as

$$\tau(K^-K^+) = \tau(K^-\pi^+) / (1 + y_{CP})$$

in an unbinned maximum likelihood fit. This method allows us to properly estimate correlated systematic errors. The likelihood functions  $L = L_{K^-\pi^+}$  and  $L_{K^-K^+}$  are given by [13]

$$\begin{aligned} & L(\tau_{\text{SIG}}, S, S_{\text{tail}}, f_{\text{tail}}, \tau_{\text{BG}}, f_{\tau_{\text{BG}}}, S_{\text{BG}}, S_{\text{tail}}^{\text{BG}}, f_{\text{tail}}^{\text{BG}}) \\ &= \prod_i \left[ f_{\text{SIG}}^i \int_0^\infty dt' \frac{1}{\tau_{\text{SIG}}} e^{-\frac{t'}{\tau_{\text{SIG}}}} R(t^i - t'; \sigma_t^i, S, S_{\text{tail}}, f_{\text{tail}}) \right. \\ & \quad \left. + (1 - f_{\text{SIG}}^i) \int_0^\infty dt' \{ f_{\tau_{\text{BG}}} \frac{1}{\tau_{\text{BG}}} e^{-\frac{t'}{\tau_{\text{BG}}}} \right] \end{aligned}$$

$$+(1 - f_{\tau_{\text{BG}}})\delta(t')\}R(t^i - t'; \sigma_t^i, S_{\text{BG}}, S_{\text{tail}}^{\text{BG}}, f_{\text{tail}}^{\text{BG}})],$$

with separate parameters for  $K^-\pi^+$  and  $K^-K^+$ , giving a total of 18 parameters to fit including  $y_{CP}$ . The product is over the  $D^0$  candidates. Here,  $f_{\text{SIG}}^i$  is the probability that the candidate is signal, calculated as a function of the invariant mass, and  $\tau_{\text{SIG}}$  is the signal lifetime. The function  $R$  represents the resolution of the proper time  $t^i$ . The background proper-time distribution is modeled by a fraction  $f_{\tau_{\text{BG}}}$  ( $\sim 0.15$  for  $K^-\pi^+$  and  $\sim 0.21$  for  $K^-K^+$ ) with the effective lifetime  $\tau_{\text{BG}}$  ( $\sim 391$  fs for  $K^-\pi^+$  and  $\sim 497$  fs for  $K^-K^+$ ) and a fraction with zero lifetime represented by the Dirac delta function  $\delta(t')$ .

The resolution function  $R$ , separately for the signal and the background, is parameterized as:

$$R(t; \sigma_t, S, S_{\text{tail}}, f_{\text{tail}}) = (1 - f_{\text{tail}}) \frac{1}{\sqrt{2\pi}S\sigma_t} e^{-\frac{t^2}{2S^2\sigma_t^2}} + f_{\text{tail}} \frac{1}{\sqrt{2\pi}S_{\text{tail}}\sigma_t} e^{-\frac{t^2}{2S_{\text{tail}}^2\sigma_t^2}},$$

where  $\sigma_t$  is the proper-time error estimated candidate-by-candidate from the decay length error, and  $S$  and  $S_{\text{tail}}$  are global scaling factors that modify  $\sigma_t$  for the main and tail Gaussian distributions and  $f_{\text{tail}}$  is the fraction of the tail part. The main component is due to the SVD vertex resolution, while the tail component is due to poorly reconstructed tracks (*e.g.* tracks affected by misassociation of SVD hits, wrong SVD hit clustering or large angle multiple-scattering).

A simultaneous fit is performed to all the  $D^0$  candidates contained in the mass region within 40 MeV/ $c^2$  of the mean  $D^0$  mass. This wide range includes both the signal ( $< \pm 3\sigma$ ) and the background-dominated ( $> \pm 3\sigma$ ) regions. Figure 2 shows the results of the fit in the signal region. The solid lines show the fit and the dotted lines show the background contribution in the fit. Figure 3 shows the results of the fit in the background-dominated region and demonstrates that the background shape is well reproduced in the fit. The fit yields  $f_{\text{tail}} \sim 0.17$ ,  $S \sim 0.84$ , and  $S_{\text{tail}} \sim 1.75$  resulting in an average proper-time resolution of 215 fs for signal, while  $f_{\text{tail}}^{\text{BG}} \sim 0.06$ ,  $S_{\text{BG}} \sim 1.05$  and  $S_{\text{tail}}^{\text{BG}} \sim 4$  for background.

We obtain  $y_{CP} = (-0.2 \pm 1.0) \times 10^{-2}$  and  $\tau(K^-\pi^+) = 416.2 \pm 1.1$  fs from the fit. The fit results are corrected for small biases found in a large sample of MC events, where the reconstructed proper-time is smaller than the generated value. The difference diminishes when the effects of multiple scattering, decay in flight, or hadronic interaction are turned off in the MC simulation [14]. The bias is found to be  $-1.5 \pm 0.6$  fs for  $D^0 \rightarrow K^-\pi^+$  and  $-2.7 \pm 1.2$  fs for  $D^0 \rightarrow K^-K^+$ , resulting in a correction for  $y_{CP}$  of  $(-0.3 \pm 0.3) \times 10^{-2}$ , where errors are due to the MC sample statistics and included as a systematic error in the final result. With this correction to the fit we obtain the result  $y_{CP} = (-0.5 \pm 1.0) \times 10^{-2}$ .

The systematic uncertainties for  $y_{CP}$  are listed in Table I. Because  $y_{CP}$  is measured as a ratio of two lifetimes, many correlated systematic uncertainties in the reconstructed decay length cancel; as a result, errors in decay vertex measurement, uncertainties in the IP profile and the uncertainty of the reconstructed  $D^0$  momentum vector all make negligible contributions to the uncertainty of  $y_{CP}$ . A MC simulation study shows that the fit yields a signal lifetime slightly longer than the generated one due to the presence of the background. This bias is common to the  $K^-\pi^+$  and  $K^-K^+$  decays in sign and magnitude ( $\sim +3$  fs) and, therefore, has no effect on the value of  $y_{CP}$ .

A difference in the signal purity between the  $K^-\pi^+$  and  $K^-K^+$  decays may result in a bias in  $y_{CP}$ . We estimate this uncertainty by repeating the analysis for  $D^0$  samples obtained by varying

requirements for particle identification and the fit quality of the  $D^0$  decay vertex, both of which are very effective for suppressing background. The systematic uncertainty due to the background proper-time distribution is estimated by varying the  $D^0$  mass range used in the fit from the nominal  $\pm 40 \text{ MeV}/c^2$  to  $\pm 35 \text{ MeV}/c^2$  and to  $\pm 45 \text{ MeV}/c^2$ .

The systematic error originating from a correlation between the proper-time measurement and the measured  $D^0$  mass is estimated by a MC simulation study. We estimate the systematic uncertainty due to  $D^0$  candidates with large proper times ( $t > 10\tau_{D^0}$ ) by varying the  $t$  range for the fit and taking the maximum excursion to be the systematic error. Also included are the effects of the systematic uncertainties due to the statistical uncertainty of the signal probability  $f_{\text{SIG}}$  and the error of the world average value of the  $D^0$  mass [12]. The total systematic error is calculated by taking a quadratic sum of all contributions and is  $^{+0.007}_{-0.008}$ .

In summary, we have measured the  $D^0$ - $\bar{D}^0$  mixing parameter  $y_{CP}$ , using  $23.4 \text{ fb}^{-1}$  of data collected near the  $\Upsilon(4S)$  resonance, to be

$$y_{CP} = \left( -0.5 \pm 1.0^{+0.7}_{-0.8} \right) \times 10^{-2}.$$

This corresponds to a 95% confidence interval  $-0.030 < y_{CP} < 0.020$ . The result is consistent with zero and the Standard Model expectation that  $y_{CP}$  is small.

We wish to thank the KEKB accelerator group for the excellent operation of the KEKB accelerator. We acknowledge support from the Ministry of Education, Culture, Sports, Science and Technology of Japan and the Japan Society for the Promotion of Science; the Australian Research Council and the Australian Department of Industry, Science and Resources; the Department of Science and Technology of India; the BK21 program of the Ministry of Education of Korea and the SRC program of the Korea Science and Engineering Foundation; the Polish State Committee for Scientific Research under contract No.2P03B 17017; the Ministry of Science and Technology of Russian Federation; the National Science Council and the Ministry of Education of Taiwan; and the U.S. Department of Energy.

## REFERENCES

- [1] H. Nelson, hep-ex/9908021 and references therein.
- [2] These distributions are not single exponentials in general. Assuming a mixing parameter value  $y < 10^{-2}$ , the resulting bias is less than a few percent of  $y$  itself, and therefore negligible.
- [3] The use of  $\tau(K^-\pi^+)$ , in place of the lifetime of a true  $CP$ -neutral or  $CP$ -odd state, introduces a shift of order 10% in  $y_{CP}$ . We note, however, the  $y_{CP}$  is commonly defined as  $\tau(K^-\pi^+)/\tau(K^-K^+) - 1$  in the previous measurements and we follow their definition.
- [4] S. Bergmann, Y. Grossman, Z. Ligeti, Y. Nir and A.A. Petrov, Phys. Lett. B **486**, 418 (2000).
- [5] FOCUS Collaboration, J.M. Link *et al.*, Phys. Lett. B **485**, 62 (2000).
- [6] I.I. Bigi, N.G. Uraltsev, Nucl. Phys. **B592**, 92 (2001).
- [7] CLEO Collaboration, R. Godang *et al.*, Phys. Rev. Lett. **84**, 5038 (2000). Their measured parameter  $A_M$  can be expressed as  $A_M \sim -2\Delta$  when  $\Delta$  is small.
- [8] KEKB B Factory Design Report, KEK Report 95-7 (1995), unpublished; Y. Funakoshi *et al.*, Proc. 2000 European Particle Accelerator Conference, Vienna (2000).
- [9] Belle Collaboration, K. Abe *et al.*, KEK Progress Report 2000-4 (2000), to be published in Nucl. Inst. and Meth. A.
- [10] Charge-conjugate modes are implied throughout this Letter.
- [11] When a fill contains several runs, the beam position is recomputed for each run. In the case of very long runs, the beam position is also recalculated every  $\sim 2000$  event sample.
- [12] Particle Data Group, D.E. Groom *et al.*, Eur. Phys. J. **C15**, 1 (2000) and 2001 off-year partial update for the 2002 edition available on the PDG WWW pages (URL: <http://pdg.lbl.gov/>).
- [13] Belle Collaboration, K. Abe *et al.*, BELLE-CONF-0131, submitted as a contribution paper to 2001 Lepton Photon Conference.
- [14] The detector response is simulated using GEANT, R. Brun *et al.*, GEANT 3.21, CERN Report No. DD/EE/84-1 (1987).

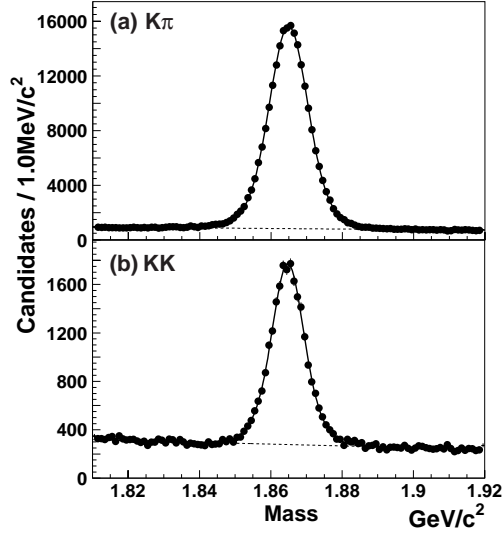


FIG. 1. The invariant mass distributions for (a)  $D^0 \rightarrow K^- \pi^+$  and (b)  $D^0 \rightarrow K^- K^+$  candidates. The results of the fit with two Gaussians (signal) and a linear function (background) are superimposed. The dotted line indicates the background.

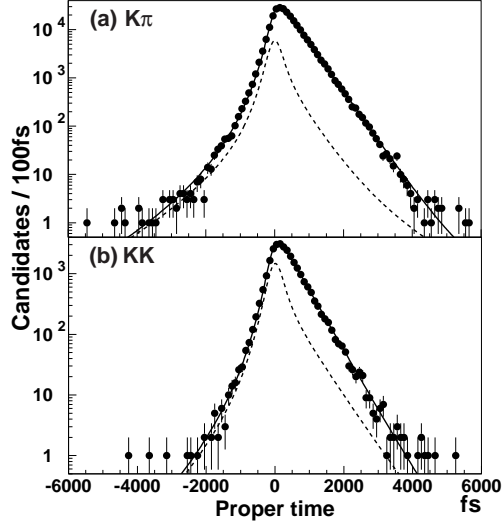


FIG. 2. Proper-time distributions and fit results for the decay modes (a)  $D^0 \rightarrow K^- \pi^+$  and (b)  $D^0 \rightarrow K^- K^+$  in the  $D^0$  mass signal region. The solid line is the result of the fit. The dotted line indicates the background contribution.

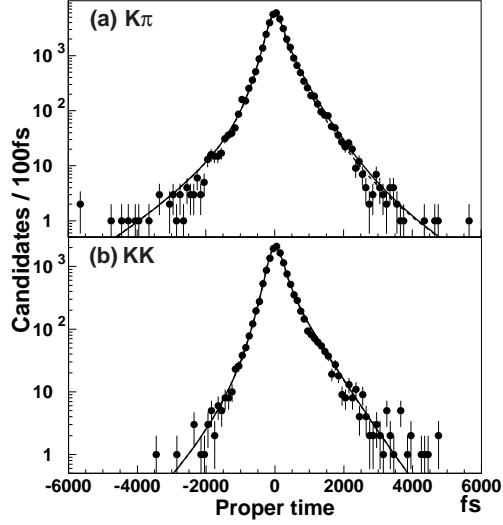


FIG. 3. Proper-time distributions and fit results for the decay modes (a)  $D^0 \rightarrow K^- \pi^+$  and (b)  $D^0 \rightarrow K^- K^+$  in the  $D^0$  mass background-dominated region.

TABLE I. Summary of systematic errors on the  $y_{CP}$  measurement.

| Source                                | Systematic error ( $10^{-2}$ ) |
|---------------------------------------|--------------------------------|
| Reconstruction bias correction        | $\pm 0.3$                      |
| Decay vertex error                    | negligible                     |
| IP profile                            | negligible                     |
| $D^0$ momentum error                  | negligible                     |
| Particle identification               | $\pm 0.5$                      |
| Decay vertex quality                  | +0.1<br>-0.4                   |
| Background $t$ distribution           | +0.2<br>-0.1                   |
| $D^0$ mass – $t$ correlation          | $\pm 0.3$                      |
| Large proper times                    | $\pm 0.2$                      |
| Signal probability $f_{\text{SIG}}^i$ | $\pm 0.1$                      |
| World average $D^0$ mass              | $\pm 0.1$                      |
| Total                                 | +0.7<br>-0.8                   |